Learning Sight from Sound: Ambient Sound Provides Supervision for Visual Learning

As Published: 10.1007/S11263-018-1083-5

Publisher: Springer Nature America, Inc

Persistent URL: https://hdl.handle.net/1721.1/135848

Version: Original manuscript: author's manuscript prior to formal peer review

Int J Comput Vis manuscript No.
(will be inserted by the editor)

Learning Sight from Sound: Ambient Sound Provides Supervision for Visual Learning

Andrew Owens · Jiajun Wu · Josh H. McDermott · William T. Freeman · Antonio Torralba

Received: date / Accepted: date

Abstract The sound of crashing waves, the roar of fast-moving cars – sound conveys important information about the objects in our surroundings. In this work, we show that ambient sounds can be used as a supervisory signal for learning visual models. To demonstrate this, we train a convolutional neural network to predict a statistical summary of the sound associated with a video frame. We show that, through this process, the network learns a representation that conveys information about objects and scenes. We evaluate this representation on several recognition tasks, finding that its performance is comparable to that of other state-of-the-art unsupervised learning methods. Finally, we show through visualizations that the network learns units that are selective to objects that are often associated with characteristic sounds. This paper extends an earlier conference paper, Owens et al (2016b), with additional experiments and discussion.

Keywords sound · convolutional networks · unsupervised learning

Andrew Owens
University of California, Berkeley
Massachusetts Institute of Technology
E-mail: andrewo@mit.edu

Jiajun Wu
Massachusetts Institute of Technology
E-mail: jiajunwu@mit.edu

Josh H. McDermott
Massachusetts Institute of Technology
E-mail: jhm@mit.edu

William T. Freeman
Massachusetts Institute of Technology
Google Research
E-mail: billf@mit.edu

Antonio Torralba
Massachusetts Institute of Technology
E-mail: torralba@csail.mit.edu

1 Introduction

Sound conveys important information about the world around us – the bustle of a café tells us that there are many people nearby, while the low-pitched roar of engine noise tells us to watch for fast-moving cars (Gaver 1993). Although sound is in some cases complementary to visual information, such as when we listen to something out of view, vision and hearing are often informative about the same structures in the world. Here we propose that as a consequence of these correlations, concurrent visual and sound information provide a rich training signal that can be used to learn useful representations of the visual world.

In particular, an algorithm trained to predict the sounds that occur within a visual scene might be expected to learn about objects and scene elements that are associated with salient and distinctive noises, such as people, cars, and flowing water (Figure 1). Such an algorithm might also learn to associate visual scenes with the ambient sound textures (McDermott and Simoncelli 2011) that occur within them. It might, for example, associate the sound of wind with outdoor scenes, and the buzz of refrigerators with indoor scenes.

Although human annotations are indisputably useful for learning, they are expensive to collect. The correspondence between ambient sounds and video is, by contrast, ubiquitous and free. While there has been much work on learning from unlabeled image data (Doersch et al 2015; Wang and Gupta 2015; Le et al 2012), an audio signal may provide information that is largely orthogonal to that available in images alone – information about semantics, events, and mechanics are all readily available from sound (Gaver 1993).

One challenge in utilizing audio-visual input is that the sounds we hear are only loosely associated with what we see. Sound-producing objects often lie outside of our visual field, and objects that are capable of producing characteristic sounds – barking dogs, ringing phones – do not always do

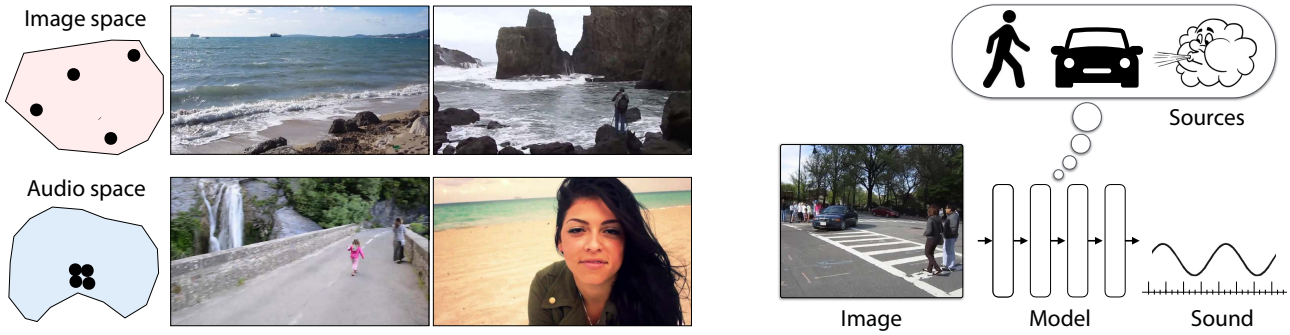

(a) Videos with similar audio tracks

(b) Audio-visual structures

Fig. 1: Predicting audio from images requires an algorithm to generalize over a variety of visual transformations. During the learning process, a sound-prediction algorithm will be forced to explain why the images in (a) are closely clustered in audio feature space. This requires detecting the water in the scene (or its close correlates, such as sand), while ignoring variations in appearance – the scene illumination, the angle of the camera, the presence of people in frame – that do not affect the sound. A sound-prediction model thus must (b) learn to recognize structures that appear in both modalities.

so. A priori it is thus not obvious what might be achieved by predicting sound from images.

In this work, we show that a model trained to predict held-out sound from video frames learns a visual representation that conveys semantically meaningful information. We formulate our sound-prediction task as a classification problem, in which we train a convolutional neural network (CNN) to predict a statistical summary of the sound that occurred at the time a video frame was recorded. We then validate that the learned representation contains significant information about objects and scenes.

We do this in two ways: first, we show that the image features that we learn through our sound-prediction task can be used for object and scene recognition. On these tasks, our features obtain performance that is competitive with that of state-of-the-art unsupervised and self-supervised learning methods. Second, we show that the intermediate layers of our CNN are highly selective for objects. This augments recent work (Zhou et al 2015) showing that object detectors "emerge" in a CNN's internal representation when it is trained to recognize scenes. As in the scene recognition task, object detectors emerge inside of our sound-prediction network. However, our model learns these detectors from an unlabeled audio-visual signal, without any explicit human annotation.

In this paper, we: (1) present a model based on visual CNNs and sound textures (McDermott and Simoncelli 2011) that predicts a video frame's held-out sound; (2) demonstrate that the CNN learns units in its convolutional layers that are selective for objects, extending the methodology of Zhou et al (2015); (3) validate the effectiveness of sound-based supervision by using the learned representation for object- and scene-recognition tasks. These results suggest that sound data, which is available in abundance from consumer videos, provides a useful training signal for visual learning.

2 Related Work

We take inspiration from work in psychology, such as Gaver's Everyday Listening (Gaver 1993), that studies the ways that humans learn about objects and events using sound. In this spirit, we would like to study the situations where sound tells us about visual objects and scenes. Work in auditory scene analysis (Ellis et al 2011; Eronen et al 2006; Lee et al 2010) meanwhile has provided computational methods for recognizing structures in audio streams. Following this work, we use a sound representation (McDermott and Simoncelli 2011) that has been applied to sound recognition (Ellis et al 2011) and synthesis tasks (McDermott and Simoncelli 2011).

The idea of learning from paired audio-visual signals has been studied extensively in cognitive science (Smith and Gasser 2005), and early work introduced computational models for these ideas. Particularly relevant is the seminal work of de Sa (de Sa 1994a,b), which introduced a self-supervised learning algorithm for jointly training audio and visual networks. Their method works on the principle of minimizing disagreement: they maintain a codebook (represented as a small neural network) that maps audio and visual examples to a label. They then iteratively refine the codebooks until they assign the same labels to each exemplar.

More recently, researchers have proposed many unsupervised learning methods that learn visual representations by solving prediction tasks (sometimes known as *pretext* tasks) for which the held-out prediction target is derived from a natural signal in the world, rather than from human annotations. This style of learning has been called *self supervision* (de Sa 1994b) or "natural" supervision (Isola 2015).

With these methods, the supervisory signal may come from video, for example by having the algorithm estimate camera motion (Agrawal et al 2015; Jayaraman and Grauman 2015) or track content across frames (Wang and Gupta 2015; Mobahi et al 2009; Goroshin et al 2015). There are also methods that learn from static images, for example by predicting the relative location of image patches (Doersch et al 2015; Isola et al 2016), or by learning invariance to simple geometric and photometric transformations (Dosovitskiy et al 2014). The assumption behind these methods is that, in order to solve the pretext task, the model will have to learn about semantics, and therefore through this process it will learn features that are broadly useful.

While we share with this work the high-level goal of learning image representations, and we use a similar technical approach, our work differs in significant ways. In contrast to methods whose supervisory signal comes entirely from the imagery itself, ours comes from a modality (sound) that is complementary to vision. This is advantageous because sound is known to be a rich source of information about objects and scenes (Gaver 1993; Ellis et al 2011), and because it is largely invariant to visual transformations, such as lighting, scene composition, and viewing angle (Figure 1). Predicting sound from images thus requires some degree of generalization to visual transformations. Moreover, our supervision task is based on solving a straightforward classification problem, which allows us to use a network design that closely resembles those used in object and scene recognition (rather than, for example, the siamese-style networks used in video methods).

Our approach is closely related to recent audio-visual work (Owens et al 2016a) that predicts soundtracks for videos that show a person striking objects with a drumstick. A key feature of this work is that the sounds are "visually indicated" by actions in video – a situation that has also been considered in other contexts, such as in the task of visually localizing a sound source (Hershey and Movellan 1999; Kidron et al 2005; Fisher III et al 2000) or in evaluating the synchronization between the two modalities (Slaney and Covell 2000). In the natural videos that we use, however, the visual motion that produces the sound may not be easily visible, and sound sources are also frequently out of frame. Also, in contrast to other recent work in multi-modal representation learning (Ngiam et al 2011; Srivastava and Salakhutdinov 2012; Andrew et al 2013), our technical approach is based on solving a self-supervised classification problem (rather than fitting a generative model or autoencoder), and our goal is to learn visual representations that are generally useful for object recognition tasks.

This work was originally introduced in a conference paper (Owens et al 2016b). In this expanded version, we include additional results. In particular: (1) a comparison between an audio representation learned from unlabeled data and "ground-truth" human-annotated audio labels (Section 6), (2) additional visualizations using class activation maps (Section 4.1), and (3) an expanded comparison of our learned image features (Section 5).

Since our original publication, researchers have proposed many interesting audio-visual learning methods. In particular, Arandjelović and Zisserman (2017) solved a similar unsupervised learning problem, but instead of using handcrafted audio features, they jointly learned audio and visual CNNs. To do this, they used an embedding-like model, whereby they trained visual and audio CNNs to predict whether a given pair of audio and visual examples were sampled from the same video. Likewise, Aytar et al (2016) introduced a method for transferring object labels from visual CNNs to audio CNNs. To do this, they used a form of cross-modal distillation (Gupta et al 2016), and trained an audio CNN to predict which semantic labels a pre-trained visual CNN will assign to a paired audio-visual example.

Researchers have also developed methods for learning from multiple self-supervision tasks (Doersch and Zisserman 2017), which could potentially be used to combined audio-based training with other methods. They have also developed a variety of new, successful self-supervised learning approaches, such as methods based on colorizing grayscale images (Zhang et al 2016, 2017) and predicting how objects move (Pathak et al 2017). We include additional comparisons with these new methods.

There has also been recent work in visualizing the internal representation of a neural net. For example, Bau et al (2017) quantified the number of object-selective units in our network, as well as other recent networks trained with self-supervised learning. This work arrived at a similar conclusion as in this work, with a different visualization methodology: namely, that the model learned units that are selective to objects.

3 Learning to predict ambient audio

We would like to train a model that, when given a frame of video, can predict its corresponding sound – a task that requires knowledge of objects and scenes, among other factors like human behavior, semantics, and culture.

3.1 Statistical sound summaries

A natural question, then, is how our model should represent sound. Perhaps the first approach that comes to mind would be to estimate a frequency spectrum at the moment in which the picture was taken, similar to Owens et al (2016a). However, this is potentially suboptimal because in natural scenes it is difficult to predict the precise timing of a sound from

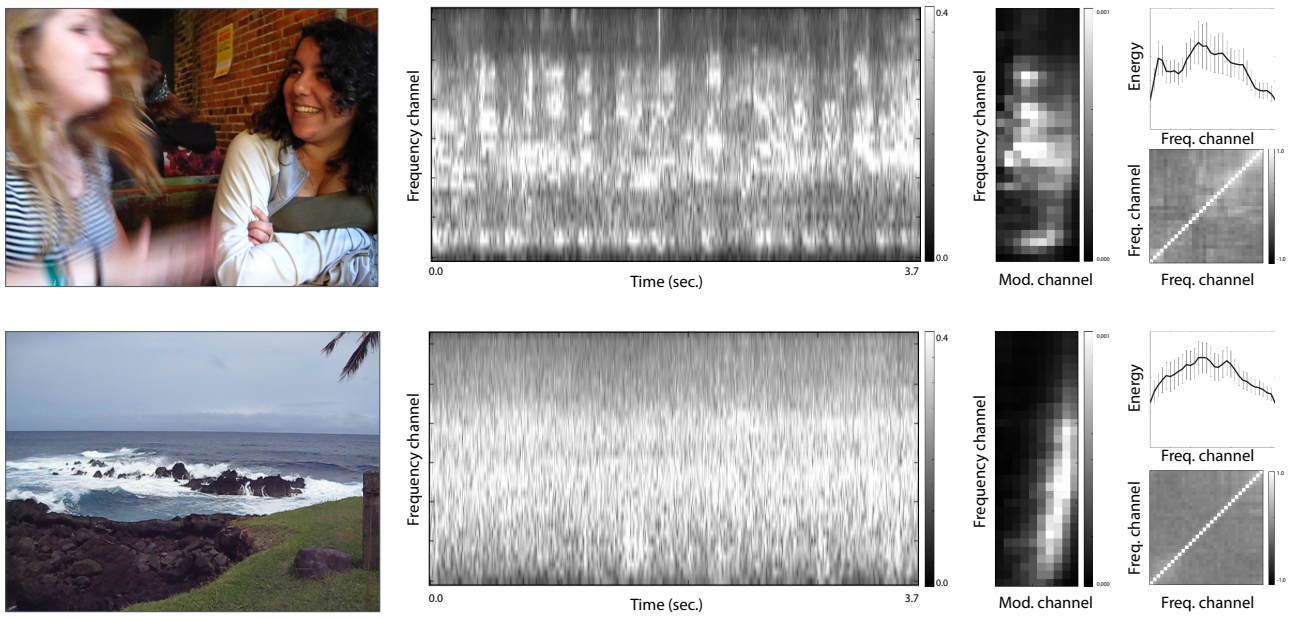

(a) Video frame (b) Cochleagram (c) Summary statistics

Fig. 2: Visual scenes are associated with characteristic sounds. Our goal is to take an image (a) and predict time-averaged summary statistics (c) of a cochleagram (b). The statistics we use are (clockwise): the response to a bank of band-pass modulation filters (sorted left-to-right in increasing order of frequency); the mean and standard deviation of each frequency band; and the correlation between bands. We show two frames from the YFCC100m dataset (Thomee et al 2015). The first contains the sound of human speech; the second contains the sound of wind and crashing waves. The differences between these sounds are reflected in their summary statistics: e.g., the water/wind sound, which is similar to white noise, contains fewer correlations between cochlear channels.

visual information. Upon seeing a crowd of people, for instance, we might expect to hear the sound of speech, but the precise timing and content of that speech might not be directly indicated by the video frames.

To be closer to the time scale of visual objects, we estimate a statistical summary of the sound, averaged over a few seconds of audio. While there are many possible audio features that could be used to compute this summary, we use the perceptually inspired sound texture model of McDermott and Simoncelli (2011), which assumes that the audio is stationary within a temporal window (we use 3.75 seconds). More specifically, we closely follow McDermott and Simoncelli (2011) and filter the audio waveform with a bank of 32 band-pass filters intended to mimic human cochlear frequency selectivity (producing a representation similar to a spectrogram). We then take the Hilbert envelope of each channel, raise each sample of the envelope to the 0.3 power (to mimic cochlear amplitude compression), and resample the compressed envelope to 400 Hz. Finally, we compute time-averaged statistics of these subband envelopes: we take the mean and standard deviation of each frequency channel, the mean squared response of each of a bank of modulation filters applied to each channel, and the Pearson correlation between pairs of channels. For the modulation filters, we use a bank of 10 band-pass filters with center frequencies ranging from 0.5 to 200 Hz, equally spaced on a logarithmic scale.

To make the sound features more invariant to gain (e.g., from the microphone), we divide the envelopes by the median energy (median vector norm) over all timesteps, and include this energy as a feature. As in McDermott and Simoncelli (2011), we normalize the standard deviation of each cochlear channel by its mean, and each modulation power by its standard deviation. We then rescale each kind of texture feature (i.e. marginal moments, correlations, modulation power, energy) inversely with the number of dimensions. The sound texture for each image is a 502-dimensional vector. In Figure 2, we give examples of these summary statistics for two audio clips. We provide more details about our audio representation in Section A.

3.2 Predicting ambient sound from images

We would like to predict sound textures from images – a task that we hypothesize leads to learning useful visual representations. Although multiple frames are available, we predict sound from a single frame, so that the learned image fea-

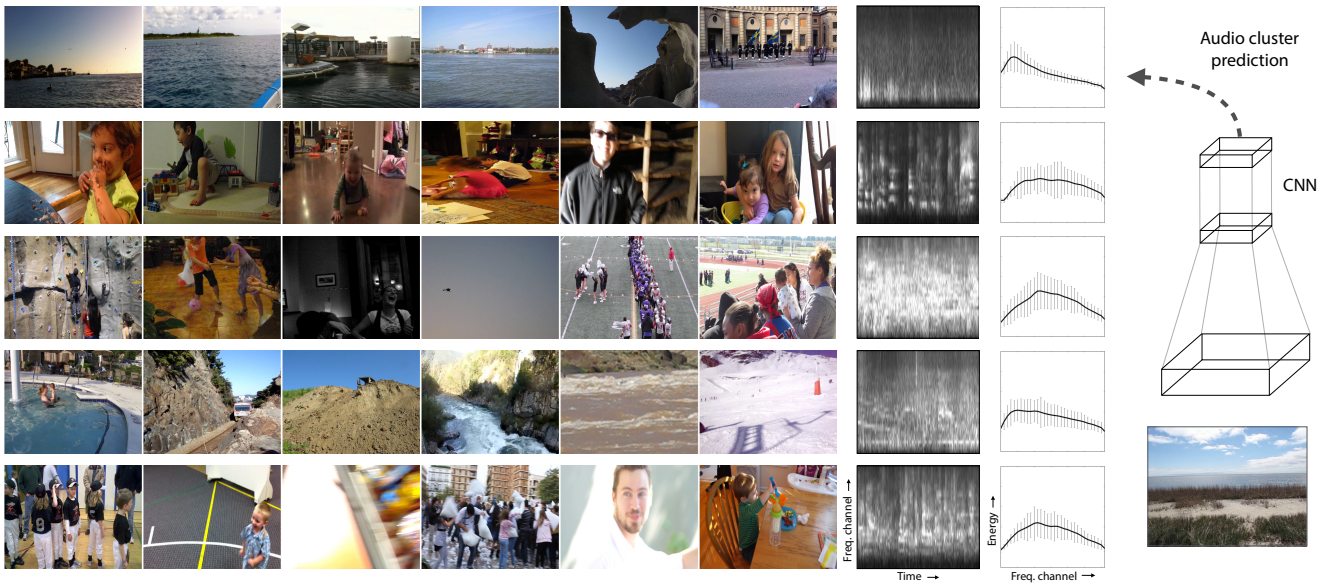

(a) Images grouped by audio cluster (b) Clustered audio stats. (c) CNN model

Fig. 3: Visualization of some of the audio clusters used in our model (5 of 30 clusters). For each cluster, we show (a) the images in the test set whose sound textures were closest to the centroid (no more than one frame per video), and (b) we visualize aspects of the sound texture used to define the cluster centroid – specifically, the mean and standard deviation of the frequency channels. We also include a representative cochleagram (that of the leftmost image). Although the clusters were defined using audio, there are common objects and scene attributes in many of the images. We train a CNN to predict a video frame's auditory cluster assignment (c).

tures will be more likely to transfer to single-image recognition tasks. Furthermore, since the actions that produce the sounds may not appear on screen, motion information may not always be applicable.

While one option would be to regress the sound texture v_j directly from the corresponding image I_j, we choose instead to define explicit sound categories and formulate this visual recognition problem as a classification task. This also makes it easier to analyze the network, because it allows us to compare the internal representation of our model to object- and scene-classification models with similar network architecture (Section 4). We consider two labeling models: one based on a vector quantization, the other based on a binary coding scheme.

Clustering audio features In the *Clustering* model, the sound textures $\{v_j\}$ in the training set are clustered using k-means. These clusters define image categories: we label each sound texture with the index of the closest centroid, and train our CNN to label images with their corresponding labels.

We found that audio clips that belong to a cluster often contain common objects. In Figure 3, we show examples of such clusters, and in the supplementary material we provide their corresponding audio. We can see that there is a cluster that contains indoor scenes with children in them; these are relatively quiet scenes punctuated with speech sounds. Another cluster contains the sounds of many people speaking at once (often large crowds); another contains many water scenes (usually containing loud wind sounds). Several clusters capture general scene attributes, such as outdoor scenes with light wind sounds. During training, we remove examples that are far from the centroid of their cluster (more than the median distance to the vector, amongst all examples in the dataset).

Binary coding model For the other variation of our model (which we call the *Binary* model), we use a binary coding scheme (Indyk and Motwani 1998; Salakhutdinov and Hinton 2009; Weiss et al 2009) equivalent to a multi-label classification problem. We project each sound texture v_j onto the top principal components (we use 30 projections), and convert these projections into a binary code by thresholding them. We predict this binary code using a sigmoid layer, and during training we measure error using cross-entropy loss.

For comparison, we also trained a model (which we call the *Spectrum* model) to approximately predict the frequency spectrum at the time that the photo was taken, in lieu of a full sound texture. Specifically, for our sound vectors v_j in this model, we used the mean value of each cochlear channel within a 33.3 ms interval centered on the input frame (ap-

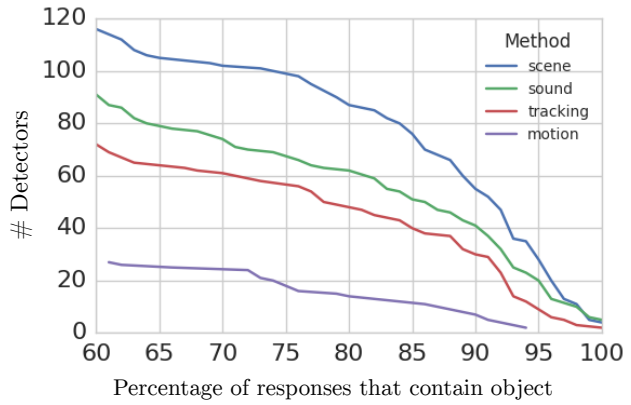

Fig. 4: The number of object-selective units for each method, as we increase the threshold used to determine whether a unit is object-selective. This threshold corresponds to the fraction of images that contain the object in question, amongst the images with the 60 largest activations. For our analysis in Section 4, we used a threshold of 60%.

proximately one frame of a 30 Hz video). For training, we used the projection scheme from the Binary model.

Training We trained our models on a 360,000-video subset of the YFCC100m video dataset (Thomee et al 2015) (which we also call the *Flickr video* dataset). A large fraction of the videos in the dataset are personal video recordings containing natural audio, though many were post-processed, e.g. with added subtitles, title screens, and music. We divided our videos into training and test sets, and we randomly sampled 10 frames per video (1.8 million training images total). For our network architecture, we used the CaffeNet architecture (Jia et al 2014), a variation of Krizhevsky et al (2012), with batch normalization (Ioffe and Szegedy 2015). We trained our model with Caffe (Jia et al 2014), using a batch size of 256, for 320,000 iterations of stochastic gradient descent with momentum, decreasing the learning rate from an initial value of 0.01 by a factor of 10 every 100,000 iterations.

4 What does the network learn to detect?

We evaluate the image representation that our model learned in multiple ways. First, we demonstrate that the internal representation of our model contains convolutional units (i.e., neurons) that are selective to particular objects, and we analyze those objects' distribution. We then empirically evaluate the quality of the learned representation for several image recognition tasks, finding that it achieves performance comparable to other feature-learning methods that were trained without human annotations.

Previous work (Zhou et al 2015) has shown that a CNN trained to predict scene categories will learn convolutional units that are selective for objects – a result that follows naturally from the fact that scenes are often defined by the objects that compose them. We ask whether a model trained to predict ambient sound, rather than explicit human labels, would learn object-selective units as well. For these experiments, we used the Clustering variation of our model, because the structure of the network is the same as the scene-recognition model used in Zhou et al (2015) (whereas the Binary model differs in that it solves a multi-label prediction problem).

Labeling object-selective units Following Zhou et al (2015), we visualized the images that each neuron in the top convolutional layer (conv5) responded most strongly to. To do this, we sampled a pool of 200,000 images from our Flickr video test set. We then collected, for each convolutional unit, the 60 images in this set that gave the unit the largest activation. Next, we applied the visualization technique of Zhou et al (2015) to approximately superimpose the unit's receptive field onto the image. Specifically, we found all of the spatial locations in the layer for which the unit's activation strength was at least half that of its maximum response. We then masked out the parts of the image that were not covered by the receptive field of one of these high-responding spatial units. We assumed a circular receptive field, obtaining its radius from Zhou et al (2015).

We then labeled the neurons by showing the masked images to human annotators on Amazon Mechanical Turk (three per unit), asking them: (1) whether an object is present in many of these regions, and if so, what it is; (2) to mark the images whose activations contain these objects. Unlike Zhou et al (2015), we only searched for units that were selective to objects, and did not allow labels for textures or other low-level image structure. For each unit, if at least 60% of its top 60 activations contained the object in question, we considered it to be *selective* for the object (or, following Zhou et al (2015), we say that it is a *detector* for that object). We (an author) then assigned an object name to the unit, using the category names provided by the SUN database (Xiao et al 2010).

We found that 91 of the 256 units in our model were object-selective in this way, and we show a selection of them in Figure 5 (additional examples are provided in Figure 14). In Figure 4, we study how the number of object-selective units changes as we make our evaluation criteria more stringent, by increasing the 60% threshold.

Explaining which objects emerge We compared the number of object-selective units to those of a CNN trained to recognize human-labeled scene categories on Places (Zhou et al 2015). As expected, this model – having been trained

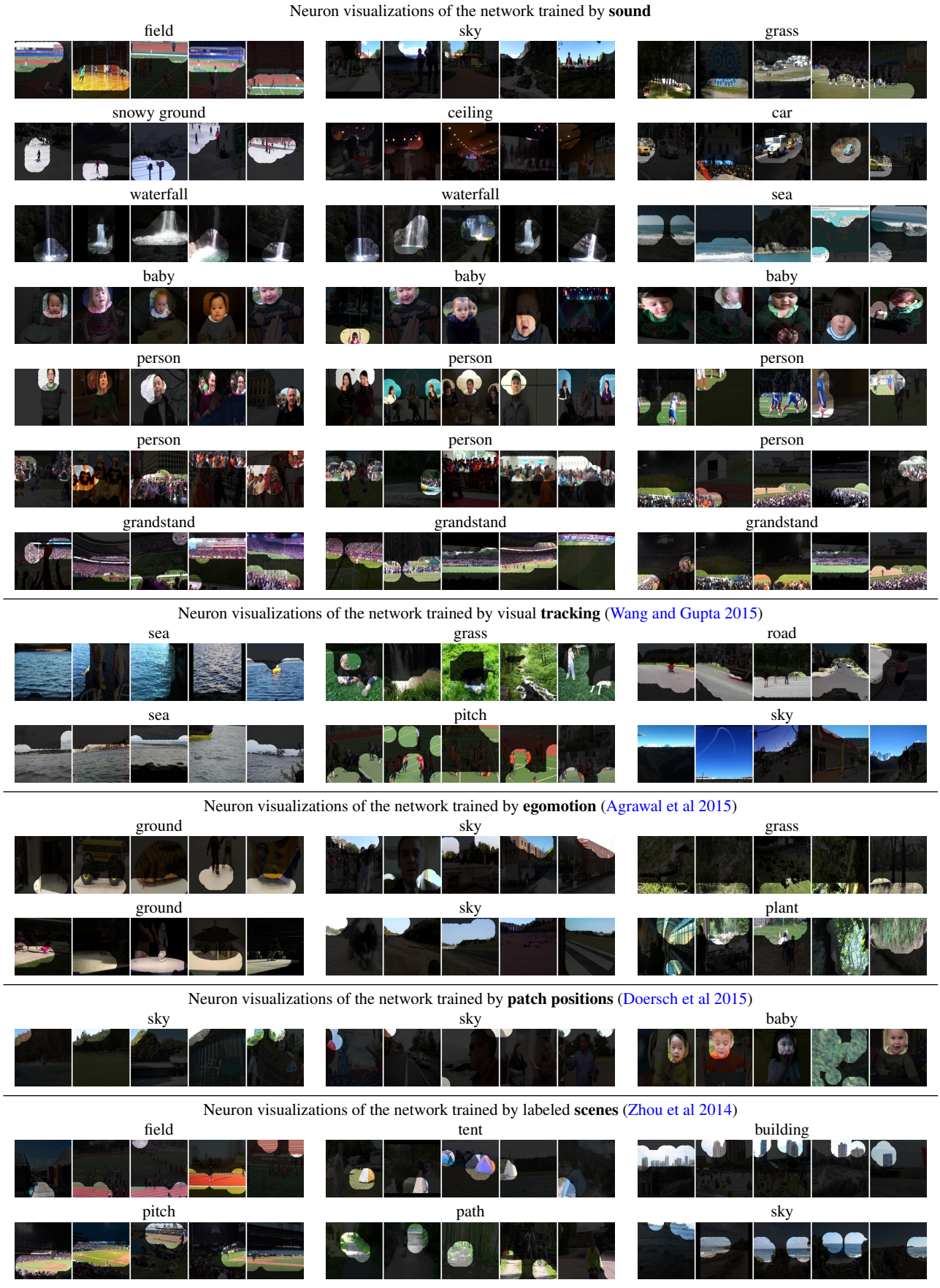

Fig. 5: Top 5 responses for convolutional units in various networks, evaluated on videos from the YFCC100m dataset.

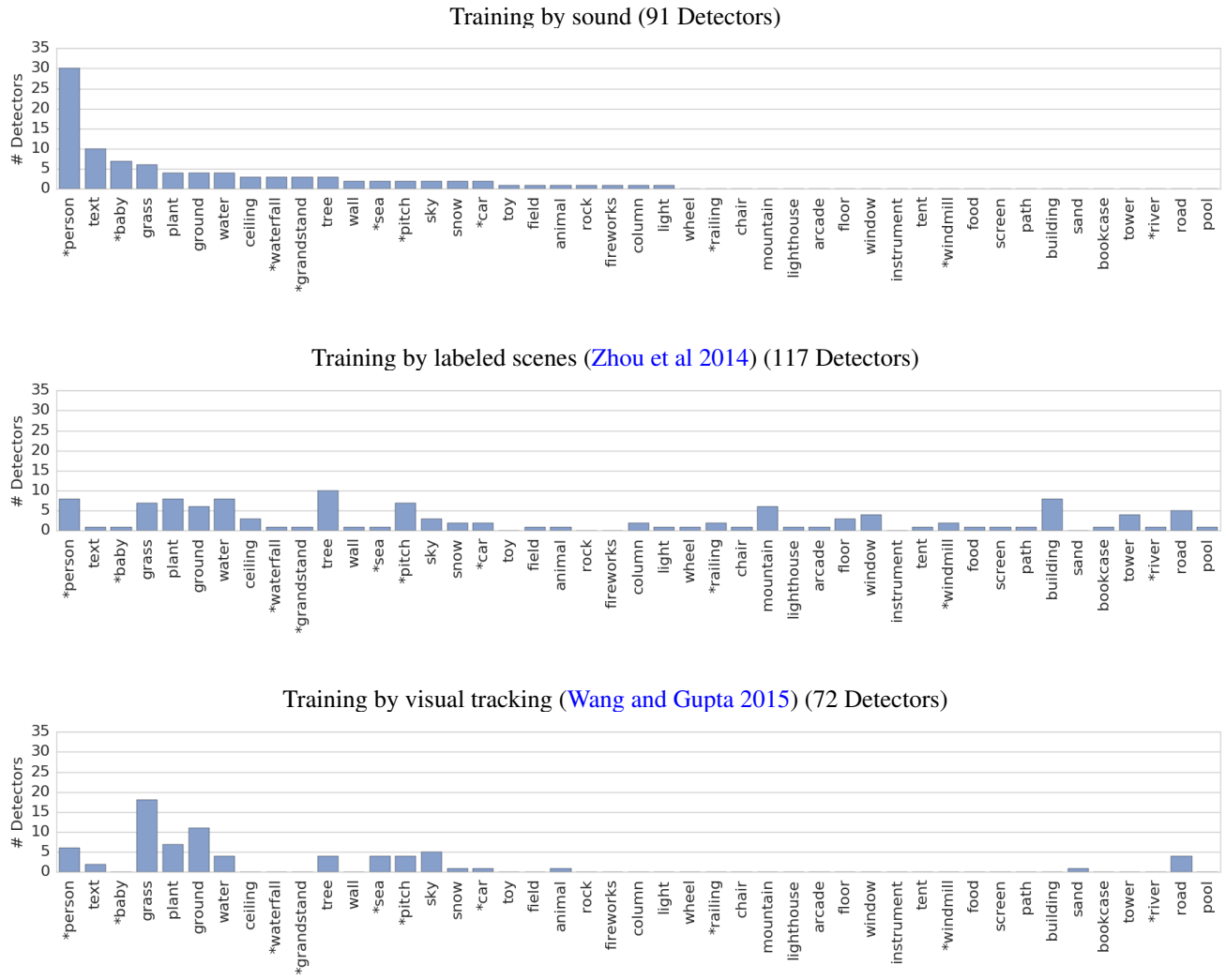

Fig. 6: Histogram of object-selective units in networks trained with different styles of supervision. From top to bottom: training to predict ambient sound (our Clustering model); training to predict scene category using the Places dataset (Zhou et al 2014); and training to do visual tracking (Wang and Gupta 2015). Compared to the tracking model, which was also trained without semantic labels, our network learns more high-level object detectors. It also has more detectors for objects that make characteristic sounds, such as *person*, *baby*, and *waterfall*, in comparison to the one trained on Places. Categories marked with $*$ are those that we consider to make characteristic sounds.

Method	Sound	Places
# Detectors	91	117
# Detectors for objects with characteristic sounds	49	26
Videos with object sound	43.7%	16.9%
Characteristic sound rate	81.2%	75.9%

Table 1: Row 1: the number of detectors (i.e. units that are selective to a particular object); row 2: the number of detectors for objects with characteristic sounds; row 3: fraction of videos in which an object's sound is audible (computed only for object classes with characteristic sounds); row 4: given that an activation corresponds to an object with a characteristic sound, the probability that its sound is audible. There are 256 units in total for each method.

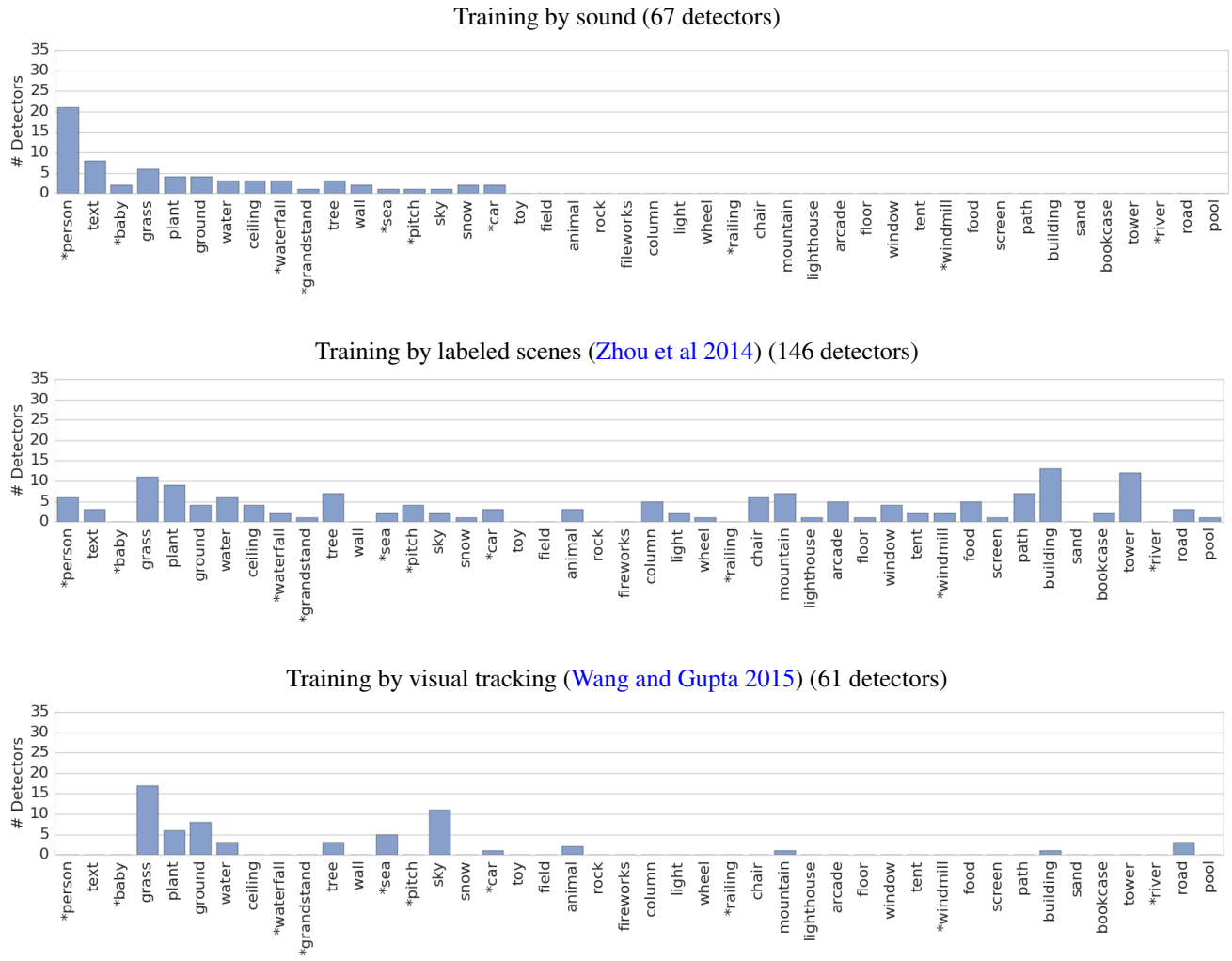

Fig. 7: The number of object-selective per category, when evaluating the model on the SUN and ImageNet datasets (cf. Figure 6, in which the models were evaluated on the YFCC100m video dataset).

Fig. 8: A selection of object-selective neurons, obtained by testing our model on the SUN and ImageNet datasets. We show the top 5 activations for each unit.

with explicit human annotations – contained significantly more such units (117 units). We also asked whether object-selective neurons appear in the convolutional layers when a CNN is trained on other tasks that do not use human labels. As a simple comparison, we applied the same methodology to the egomotion-based model of Agrawal et al (2015) and to the tracking-based method of Wang and Gupta (2015). We applied these networks to large crops (in all cases resizing the input image to 256×256 pixels and taking the center 227×227 crop), though we note that they were originally trained on significantly smaller cropped regions.

Do different kinds of self-supervision lead to different kinds of object selectivity? Using the unit visualization method, we found that the tracking-based model also learned object-selective units, but that the objects that it detected were often textural "stuff," such as grass, ground, and water, and

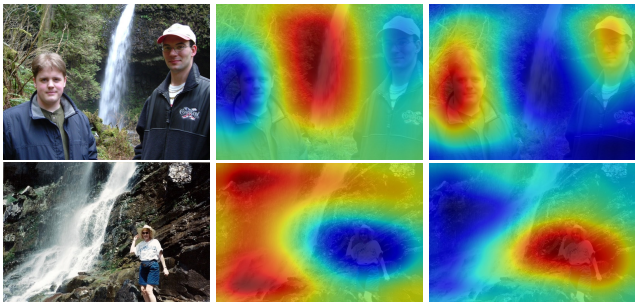

Fig. 9: Class activation maps (CAMs) for speech and flowing water sounds. The categories correspond to the third and fifth examples in Figure 10. The CAM is colored such that red corresponds to high probability of an audio category.

that there were fewer of these detection units in total (72 of 256). The results were similar for the egomotion-based model, which had 27 such units. In Figure 6, we provide the distribution of the objects that the units were selective to. We also visualized neurons from the method of Doersch et al (2015) (as before, applying the network to whole images, rather than to patches). We found a significant number of the units were selective for position, rather than to objects. For example, one convolutional unit responded most highly to the upper-left corner of images – a unit that may be useful for the training task, which involves predicting the relative position of image patches (moreover, Doersch et al (2015) suggests that the model uses low-level cues, such as chromatic aberration, rather than semantics). In Figure 5, we show visualizations of a selection of object-detecting neurons for all of these methods.

The differences between the objects detected by these methods and our own may have to do with the requirements of the tasks being solved. The other unsupervised methods, for example, all involve comparing multiple input images or cropped regions in a relatively fine-grained way. This may correspondingly change the representation that the network learns in its last convolutional layer – requiring its units to encode, say, color and geometric transformations rather than object identities. Moreover, these networks may represent semantic information in other (more distributed) ways that would not necessarily be revealed through this visualization method.

Next, we asked what kinds of objects our network learned to detect. We hypothesized that the object-selective neurons were more likely to respond to objects that produce (or are closely associated with) characteristic sounds[1]. To evaluate this, we (an author) labeled the SUN object categories according to whether they were closely associated with a characteristic sound in the videos that contained the top detections. We denote these categories with a $*$ in Figure 6. We found that some objects, such as fireworks, were usually associated in these videos with the sound of wind or human speech, rather the sound of the object itself. We therefore chose not to count these as objects associated with characteristic sounds. Next, we counted the number of units that were selective to these objects, finding that our model contained significantly more such units than a scene-recognition network trained on the Places dataset, both in total number and as a proportion (Table 1). A significant fraction of these units were selective to people (adults, babies, and crowds).

Analyzing the types of objects that were detected Finally, we asked whether the sounds that these objects make were actually present in the videos that these video frames were sampled from. To do this, we listened to the sound of the top 30 video clips for each unit, and recorded whether the sound was made by the object that the neuron was selective to (e.g., human speech for the *person* category). We found that 43.7% of these videos contained the objects' sounds (Table 1).

To examine the effect of the dataset used to create the neuron visualizations, we applied the same neuron visualization technique to 200,000 images sampled equally from the SUN and ImageNet datasets (as in Zhou et al (2015)). We show examples of these neurons in Figure 8 and plot their distribution Figure 7. As expected, we found that the distribution of objects was similar to that of the YFCC100m dataset. However, there were fewer detectors in total (67 vs. 91), and there were some categories, such as *baby*, that appeared significantly less often as a fraction of the total detectors. This may be due to the differences in the underlying distribution of objects in the datasets. For example, SUN focuses on scenes and contains more objects labeled *tree*, *lamp*, and *window* than objects labeled *person* (Zhou et al 2015). We also computed a detector histogram for the model of Wang and Gupta (2015), finding that the total number of detectors was similar to the sound-based model (61 detectors), but that, as before, the dominant categories were textural "stuff" (e.g., grass, plants).

4.1 Visualizing sound predictions

These neuron visualizations suggest that our model, internally, is coding for different object categories, To more directly visualize the relationship between visual structures and sound categories, we trained a variation of our model to predict a class activation map (CAM) (Zhou et al 2016). Following Zhou et al (2016), we replaced the fully connected layers of our model with convolutions whose activations are spatially averaged to produce class probabilities (i.e. using global average pooling (Lin et al 2014)). Under

[1] For conciseness, we sometimes call these "sound-making" objects, even if they are not literally the source of the sound.

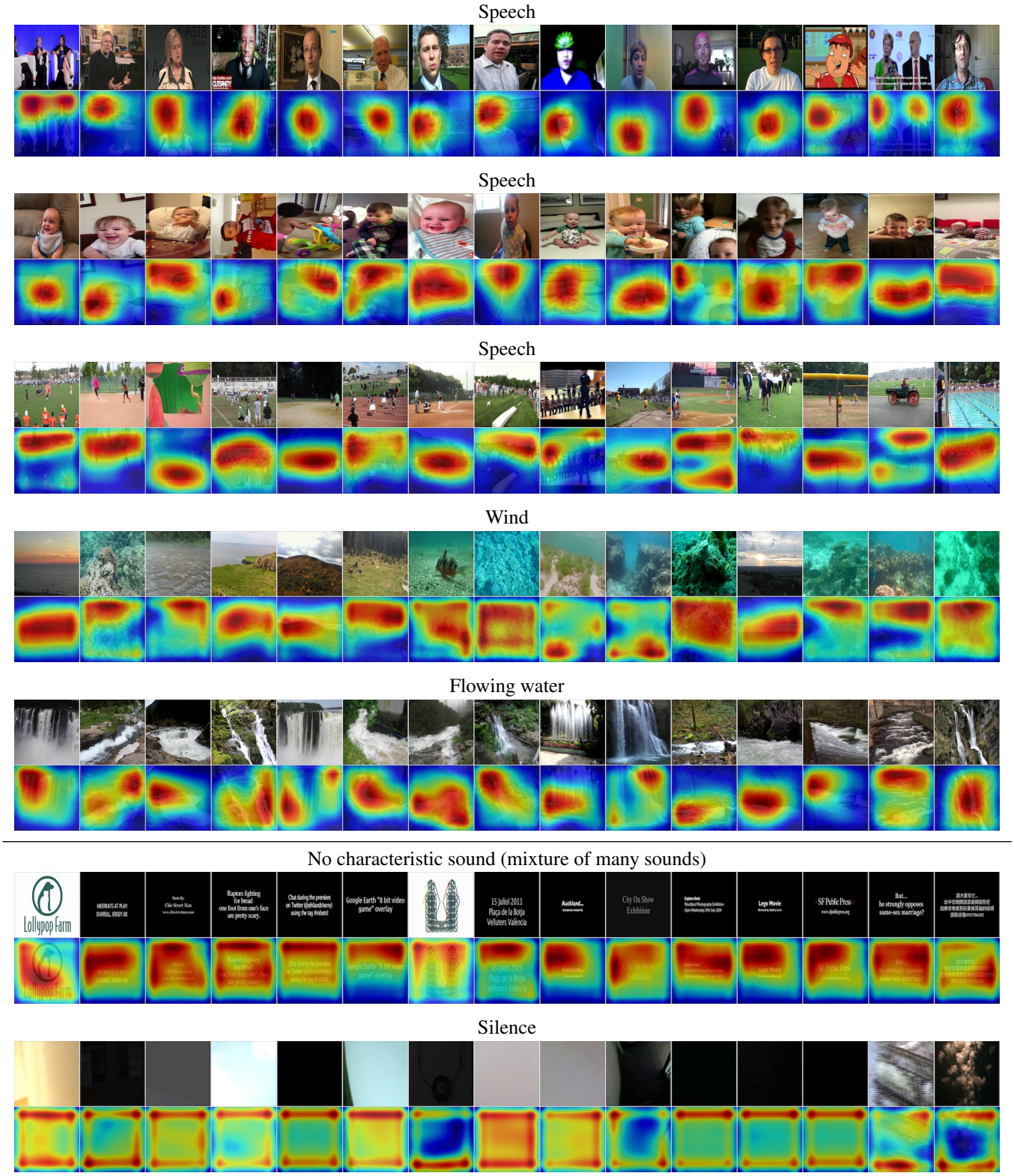

Fig. 10: For 7 (of 30) audio categories, we show the network's most confident predictions and their CAMs, and we provide a description of their sound. We show results from the YFCC100m video dataset (to avoid having redundant images from similar videos, we show for each category at most one example per Flickr user).

this model, each spatial position independently casts a vote for each sound category. These spatial votes, then, can be used to localize the visual structures that the network is detecting.

In Figure 10 we show, for 7 of 30 audio classes, the images for which our model assigned the highest probability, along with their corresponding CAMs (displayed as heat maps). We also provide a qualitative description for the audio categories, which we (an author) obtained by listening to the audio clips that are nearest to its centroid (similar to Section 3). Together, these visualizations help to link visual structures with sound. We see, for example, that speech sounds often correspond to faces, while flowing water sounds correspond to waterfalls. In Figure 9 we also show qualitative examples where CAM visualizations from two different audio categories – one corresponding to speech, another to flowing water sounds – localized two different object types.

5 Evaluating the image representation

We have seen through visualizations that a CNN trained to predict sound from an image learns units that are selective for objects. Now we evaluate how well this representation conveys information about objects and scenes.

5.1 Recognizing objects and scenes

Since our goal is to measure the amount of semantic information provided by the learned representation, rather than to seek absolute performance, we used a simple evaluation scheme. In most experiments, we computed image features using our CNN and trained a linear SVM to predict object or scene category using the activations in the top layers.

Object recognition First, we used our CNN features for object recognition on the PASCAL VOC 2007 dataset (Everingham et al 2010). We trained a one-vs.-rest linear SVM to detect the presence of each of the 20 object categories in the dataset, using the activations of the upper layers of the network as the feature set (pool5, fc6, and fc7). To help understand whether the convolutional units considered in Section 4 directly convey semantics, we also created a global max-pooling feature (similar to Oquab et al (2015)), where we applied max pooling over the entire convolutional layer. This produces a 256-dimensional vector that contains the maximum response of each convolutional unit (which we refer to as *max5*). Following common practice, we evaluated the network on a center 227×227 crop of each image (after resizing the image to 256×256), and we evaluated the results using mean average precision (mAP). We chose the SVM regularization parameter for each method by maximizing mAP on the validation set using grid search (we used $\{0.5^k \mid 4 \leq k < 20\}$).

The other unsupervised (or self-supervised) models in our comparison (Doersch et al 2015; Agrawal et al 2015; Wang and Gupta 2015; Zhang et al 2016; Pathak et al 2017) use different network designs. In particular, Doersch et al (2015) was trained on image patches, so following their experiments we resized its convolutional layers for 227×227 images and removed the model's fully connected layers[2]. Also, since the model of Agrawal et al (2015) did not have a pool5 layer, we added one to it. We also considered CNNs that were trained with human annotations: object recognition on ImageNet (Deng et al 2009) and scene categories on Places (Zhou et al 2014). Finally, we considered using the k-means weight initialization method of Krähenbühl et al (2016) to set the weights of a CNN model (we call this the *K-means* model).

As shown in Table 2, we found that the overall best-performing model was the recent colorization method of Zhang et al (2016), but that the best-performing variation of our model (the binary-coding method) obtained comparable performance to the other unsupervised learning methods, such as Doersch et al (2015).

Both models based on sound textures (Clustering and Binary) outperformed the model that predicted only the frequency spectrum. This suggests that the extra time-averaged statistics from sound textures are helpful. In Table 4, we report the accuracy on a per-category basis for the model trained with pool5 features. Interestingly, the sound-based models outperformed other methods when we globally pooled the conv5 features, suggesting that the convolutional units contain a significant amount of semantic information (and are well suited to being used at this spatial scale).

Scene recognition We also evaluated our model on a scene recognition task using the SUN dataset (Xiao et al 2010), a large classification benchmark that involves recognizing 397 scene categories with 7,940 training and test images provided in multiple splits. Following Agrawal et al (2015), we averaged our classification accuracy across 3 splits, with 20 examples per scene category. We chose the linear SVM's regularization parameter for each model using 3-fold cross-validation. The results are shown in Table 2.

We found that our features' performance was slightly better than that of other unsupervised models, including the colorization and patch-based models, which may be due to the similarity of our learning task to that of scene recognition. We also found that the difference between our models was smaller than in the object-recognition case, with both

[2] As a result, this model has a larger pool5 layer than the other methods: 7 × 7 vs. 6 × 6. Likewise, the fc6 layer of Wang and Gupta (2015) is smaller (1,024 dims. vs. 4,096 dims.).

Method	VOC Cls. (%mAP)				SUN397 (%acc.)			
	max5	pool5	fc6	fc7	max5	pool5	fc6	fc7
Sound (cluster)	36.7	45.8	44.8	44.3	**17.3**	**22.9**	20.7	14.9
Sound (binary)	**39.4**	46.7	47.1	47.4	17.1	22.5	**21.3**	**21.4**
Sound (spect.)	35.8	44.0	44.4	44.4	14.6	19.5	18.6	17.7
Colorization (Zhang et al 2016)	38.8	**48.3**	**49.1**	**51.0**	16.0	20.3	21.2	18.4
Object motion (Pathak et al 2017)	32.4	40.8	31.5	23.6	12.9	15.8	7.5	3.4
Texton-CNN	28.9	37.5	35.3	32.5	10.7	15.2	11.4	7.6
K-means (Krähenbühl et al 2016)	27.5	34.8	33.9	32.1	11.6	14.9	12.8	12.4
Tracking (Wang and Gupta 2015)	33.5	42.2	42.4	40.2	14.1	18.7	16.2	15.1
Patch pos. (Doersch et al 2015)	27.7	46.7	-	-	10.0	22.4	-	-
Egomotion (Agrawal et al 2015)	22.7	31.1	-	-	9.1	11.3	-	-
ImageNet (Krizhevsky et al 2012)	**63.6**	**65.6**	**69.6**	**73.6**	29.8	34.0	37.8	37.8
Places (Zhou et al 2014)	59.0	63.2	65.3	66.2	**39.4**	**42.1**	**46.1**	**48.8**

Table 2: Mean average precision for PASCAL VOC 2007 classification, and accuracy on SUN397. Here we trained a linear SVM using the top layers of different networks. We note in Section 5 that the shape of these layers varies between networks.

Method	(%mAP)
Random init. (Krähenbühl et al 2016)	41.3
Sound (cluster)	44.1
Sound (binary)	43.3
Motion (Wang and Gupta 2015; Krähenbühl et al 2016)	47.4
Egomotion (Agrawal et al 2015; Krähenbühl et al 2016)	41.8
Patch position (Doersch et al 2015; Krähenbühl et al 2016)	46.6
Calibration + Patch (Doersch et al 2015; Krähenbühl et al 2016)	**51.1**
ImageNet (Krizhevsky et al 2012)	**57.1**
Places (Zhou et al 2014)	52.8

Table 3: Mean average precision on PASCAL VOC 2007 using Fast-RCNN (Girshick 2015). We initialized the CNN weights using those of our learned sound models.

the Clustering and Binary models obtaining performance comparable to the patch-based method with pool5 features.

Pretraining for object detection Following recent work (Wang and Gupta 2015; Doersch et al 2015; Krähenbühl et al 2016), we used our model to initialize the weights of a CNN-based object detection system, Fast R-CNN (Girshick 2015), verifying that the results improved over random initialization (Table 3). We followed the training procedure of Krähenbühl et al (2016), training for 150,000 SGD iterations with an initial learning rate of 0.002. We compared our model with other published results (we report the numbers provided by Krähenbühl et al (2016)). We found that our model performed significantly better than a randomly initialized model, as well as the method of Agrawal et al (2015), but that other models (particularly Doersch et al (2015)) worked significantly better.

We note that the network changes substantially during fine-tuning, and thus the performance is fairly dependent on the parameters used in the training procedure. Moreover all models, when fine-tuned in this way, achieve results that are close to those of a well-chosen random initialization (within 6% mAP). Recent work (Krähenbühl et al 2016; Mishkin and Matas 2015) has addressed these optimization issues by rescaling the weights of a pretrained network using a data-driven procedure. The unsupervised method with the best performance combines this rescaling method with the patch-based pretraining of Doersch et al (2015).

5.2 Audio representation

Do the predicted audio categories correlate with the presence of visual objects? To test this, we used the (log) posterior class probabilities of the CAM-based sound-prediction

Method	aer	bk	brd	bt	btl	bus	car	cat	chr	cow	din	dog	hrs	mbk	prs	pot	shp	sfa	trn	tv
Sound (cluster)	68	47	38	54	15	45	66	45	42	23	37	28	73	58	**85**	25	26	32	67	42
Sound (binary)	69	45	38	56	**16**	**47**	65	45	41	25	37	28	**74**	**61**	**85**	26	39	32	**69**	38
Sound (spect.)	65	40	35	54	14	42	63	41	39	24	32	25	72	56	81	**27**	33	28	65	40
Colorization	**70**	**50**	**45**	58	15	45	**71**	50	39	**30**	38	**41**	72	57	81	17	**42**	**41**	66	38
Tracking (Wang and Gupta 2015)	67	35	41	54	11	35	62	35	39	21	30	26	70	53	78	22	32	37	61	34
Object motion	65	39	39	50	13	33	61	36	39	24	35	28	69	49	82	14	19	34	56	31
Patch Pos. (Doersch et al 2015)	**70**	44	43	**60**	12	44	66	**52**	**44**	24	**45**	31	73	48	78	14	28	39	62	**43**
Egomotion (Agrawal et al 2015)	60	24	21	35	10	19	57	24	27	11	22	18	61	40	69	13	12	24	48	28
Texton-CNN	65	35	28	46	11	31	63	30	41	17	28	23	64	51	74	9	19	33	54	30
K-means	61	31	27	49	9	27	58	34	36	12	25	21	64	38	70	18	14	25	51	25
ImageNet (Krizhevsky et al 2012)	79	**71**	**73**	75	**25**	60	80	**75**	51	**45**	60	**70**	**80**	**72**	**91**	42	**62**	56	82	62
Places (Zhou et al 2014)	**83**	60	56	**80**	23	**66**	**84**	54	**57**	40	**74**	41	**80**	68	90	**50**	45	**61**	**88**	**63**
Audio class probability	25	6	12	14	8	6	28	15	21	5	12	15	10	7	75	7	4	9	10	8

Table 4: Per-class AP scores for the VOC 2007 classification task with pool5 features (corresponds to mAP in (a)). We also show the performance obtained using the predicted log-probability of each audio category, using the CAM-based model (Section 4.1).

network as (30-dimensional) feature vectors for object recognition. While the overall performance, unsurprisingly, is low (14.7% mAP), we found that the model was relatively good at recognizing people – perhaps because so many audio categories correspond to speech. Its performance (75% AP) was similar to that of the much higher-dimensional pool5 features of the Doersch et al (2015) network (which obtains 78% AP). We show the model's per-category recognition accuracy in Table 4.

Sound cluster prediction task We also asked how well our model learned to solve its sound prediction task. We found that on our test set, the clustering-based model (with 30 clusters) chose the correct sound label 15.8% of the time. Pure chance in this case is 3.3%, while the baseline of choosing the most commonly occurring label is 6.6%.

Number of clusters We also investigated how the number of clusters (i.e. audio categories) used in constructing the audio representation affected the quality of the visual features. In Figure 11, we varied the number of clusters, finding that there is a small improvement from increasing it beyond 30, and a substantial decrease in performance when using just two clusters. We note that, due to the way that we remove examples whose audio features are not well-represented by any cluster (Section 3.2), the models with small numbers of clusters were effectively trained with fewer examples – a trade-off between cluster purity and data quantity that may affect performance of these models.

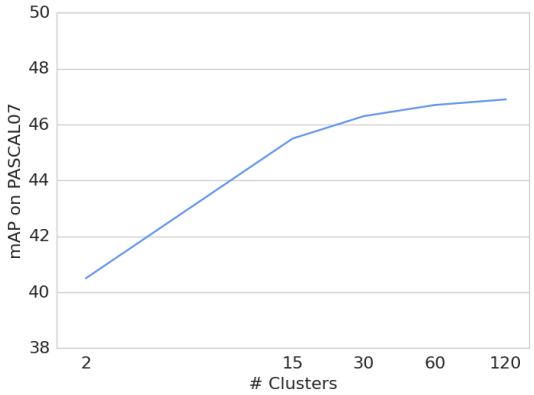

Fig. 11: Object recognition performance (recognition performance on PASCAL VOC2007) increases with the number of clusters used to define the audio label space. For our experiments, we used 30 clusters.

6 Studying the role of audio supervision

It is natural to ask what role audio plays in the learning process. Perhaps, for example, our learning algorithm would work equally well if we replaced the hand-crafted sound features with hand-crafted *visual* features, computed from the images themselves. To study this, we replaced our sound texture features with (512-dimensional) visual texton histograms (Leung and Malik 2001), using the parameters from Xiao et al (2010), and we used them to train a variation of our clustering-based model.

As expected, the images that belong to each cluster are visually coherent, and share common objects. However, we found that the network performed significantly worse than

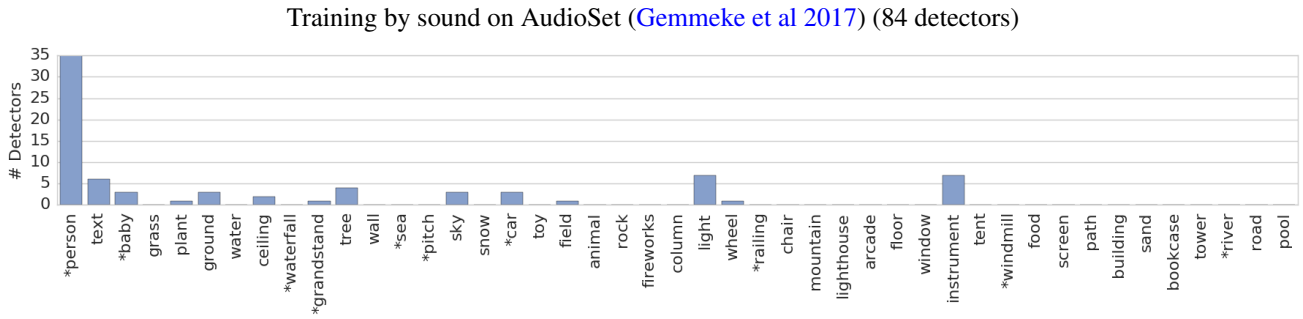

Fig. 12: We quantify the number of object-selective units for our Cluster method trained on AudioSet (Gemmeke et al 2017). As before, we visualize the units using the Flickr video dataset (cf. Figure 6).

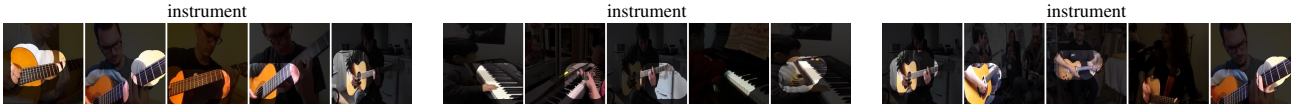

Fig. 13: Object-selective neurons for a new category (instrument), obtained by training our model on AudioSet (Gemmeke et al 2017). We show the top 5 activations for each unit.

Method	VOC Cls. (%mAP)			
	max5	pool5	fc6	fc7
Annotations	**48.8**	**55.6**	**56.3**	**58.1**
Binary	38.5	48.6	47.7	49.3
Cluster (30 clusters)	38.2	47.5	45.9	46.1
Cluster (120 clusters)	40.3	48.8	47.3	48.4
ImageNet	63.6	65.6	69.6	73.6

Table 5: Comparison between a model trained to predict ground-truth sound annotations and our unsupervised models, all trained on AudioSet (Gemmeke et al 2017). As in Section 5, we report mean average precision for PASCAL VOC 2007 classification, after training a linear SVM on the feature activations of different layers.

the audio-based method on the object- and scene-recognition metrics (Table 2). Moreover, we found that its convolutional units rarely were selective for objects (generally they responded responded to "stuff" such as grass and water).

Likely this large difference in performance is due to the network learning to approximate the texton features, obtaining low labeling error without high-level generalization. In contrast, the audio-based labels – despite also being based on another form of hand-crafted feature – are largely invariant to visual transformations, such as lighting and scale, and therefore predicting them requires some degree of generalization. This is one benefit of training with multiple, complementary modalities (as explained in Figure 1).

6.1 Human-annotated sounds

Ideally, the audio clustering procedure would produce clusters that map one-to-one with sound sources. In practice, however, the relationship between sound categories and cluster membership is significantly messier (Figure 3).

We asked what would happen if, instead of labeling the sound using a clustering procedure, we were to use "ground-truth" audio annotations provided by humans. To study this, we trained a model to predict audio categories from videos in the AudioSet dataset (Gemmeke et al 2017). The videos in this dataset contain 527 sound categories, such as *music*, *speech*, *vehicle*, *animal*, and *explosion*. From this dataset, we sampled 962,892 ten-second videos and extracted the middle frame from each one. We then trained a network (similar in structure to the Binary model) to predict the audio labels. For comparison, we also retrained our audio-based models on this data.

We found, first, that the model that used human annotations performed well (Table 5): its features performed significantly better than the state-of-the-art unsupervised methods, while still lagging behind ImageNet-based training. Second, we found that it substantially outperformed our unsupervised models trained on the same dataset. This suggests that there is substantial room for improvement by choosing audio representations that better capture semantics.

We note that the AudioSet labels may implicitly make use of visual information, both through the use of human annotators (who watched the videos during the labeling process) and due to the fact that visual classifiers were used as an input during the collection process. As such, the annotations may be best viewed as an upper bound on what is

achievable from methods that derive their supervision purely from audio.

To study the difference between the internal representation of a model learned on (unlabeled) videos in AudioSet, and those of a model trained on the YFCC100m video dataset (Flickr videos), we quantified the object-selective units (Figure 12). As before, we performed this comparison using the unsupervised *Cluster* model. While there were many similarities between the networks, such as the fact that both have a large number of units tuned to human faces, there are also significant differences. One such difference is the large number of units that are selective to musical instruments (Figure 13), which likely emerge due to the large number of music and instrument-related categories in AudioSet.

7 Discussion

Sound has many properties that make it useful as a supervisory training signal: it is abundantly available without human annotations, and it is known to convey information about objects and scenes. It is also complementary to visual information, and may therefore convey information not easily obtainable from unlabeled image analysis.

In this work, we proposed using ambient sound to learn visual representations. We introduced a model, based on convolutional neural networks, that predicts a statistical sound summary from a video frame. We then showed, with visualizations and experiments on recognition tasks, that the resulting image representation contains information about objects and scenes.

Here we considered one audio representation, based on sound textures, which led to a model capable of detecting certain objects, such as people and waterfalls. It is natural to ask whether a better audio representation would lead the model to learn about other objects. Ideally, one should jointly learn the audio representation with the visual representation – an approach taken in recent work (Arandjelović and Zisserman 2017). More broadly, we would like to know which visual objects one can learn to detect through sound-based training, and we see our work as a step in this direction.

Acknowledgments This work was supported by NSF grants #1524817 to A.T; NSF grants #1447476 and #1212849 to W.F.; a McDonnell Scholar Award to J.H.M.; and a Microsoft Ph.D. Fellowship to A.O. It was also supported by Shell Research, and by a donation of GPUs from NVIDIA. We thank Phillip Isola for the helpful discussions, and Carl Vondrick for sharing the data that we used in our experiments. We also thank the anonymous reviewers for their comments, which significantly improved the paper (in particular, for suggesting the comparison with texton features in Section 5).

A Sound textures

We now describe in more detail how we computed sound textures from audio clips. For this, we closely follow the work of McDermott and Simoncelli (2011).

Subband envelopes To compute the cochleagram features $\{c_i\}$, we filter the input waveform s with a bank of bandpass filters $\{f_i\}$.

$$c_i(t) = |(s * f_i) + jH(s * f_i)|, \tag{1}$$

where H is the Hilbert transform and $*$ denotes cross-correlation. We then resample the signal to 400Hz and compress it by raising each sample to the 0.3 power (examples in Figure 2).

Correlations As described in Section 3, we compute the correlation between bands using a subset of the entries in the cochlear-channel correlation matrix. Specifically, we include the correlation between channels c_j and c_k if $|j-k| \in \{1,2,3,5\}$. The result is a vector ρ of correlation values.

Modulation filters We also include modulation filter responses. To get these, we compute each band's response to a filter bank $\{m_i\}$ of 10 bandpass filters whose center frequencies are spaced logarithmically from 0.5 to 200Hz:

$$b_{ij} = \frac{1}{N}||c_i * m_j||^2, \tag{2}$$

where N is the length of the signal.

Marginal statistics We estimate marginal moments of the cochleagram features, computing the mean μ_i and standard deviation σ_i of each channel. We also estimate the loudness, l, of the sequence by taking the median of the energy at each timestep, i.e. $l = \text{median}(||c(t)||)$.

Normalization To account for global differences in gain, we normalize the cochleagram features by dividing by the loudness, l. Following McDermott and Simoncelli (2011), we normalize the modulation filter responses by the variance of the cochlear channel, computing $\tilde{b}_{ij} = \sqrt{b_{ij}/\sigma_i^2}$. Similarly, we normalize the standard deviation of each cochlear channel, computing $\tilde{\sigma}_i = \sqrt{\sigma_i^2/\mu_i^2}$. From these normalized features, we construct a sound texture vector: $[\mu, \tilde{\sigma}, \rho, \tilde{b}, l]$.

References

Agrawal P, Carreira J, Malik J (2015) Learning to see by moving. In: IEEE International Conference on Computer Vision 3, 7, 9, 12, 13, 14

Andrew G, Arora R, Bilmes JA, Livescu K (2013) Deep canonical correlation analysis. In: International Conference on Machine Learning 3

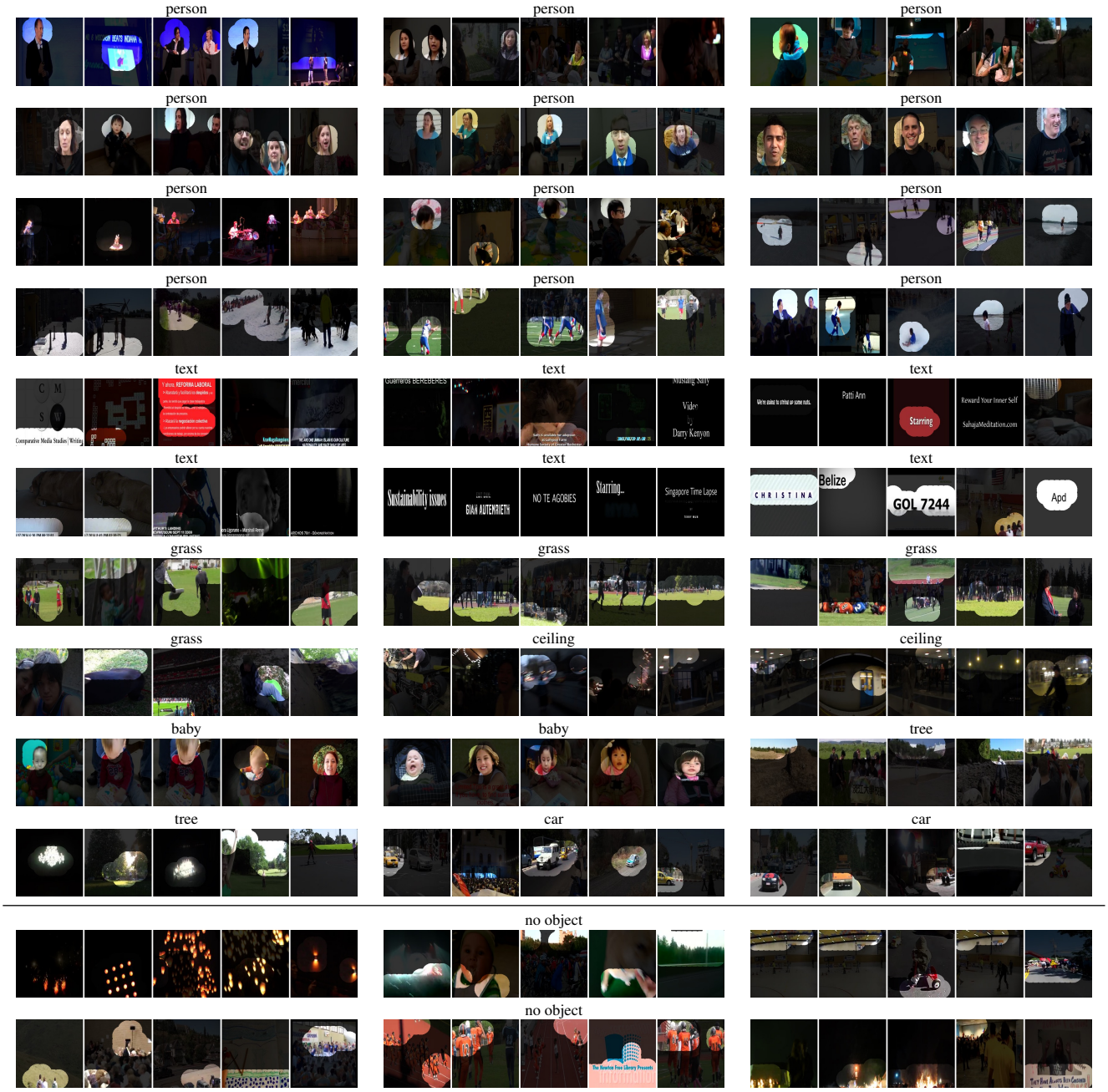

Fig. 14: Additional unit visualizations. We show the top 5 activations for units in our model (30 of 91 from common classes). The last two rows show neurons that were not selective to an object class.

Arandjelović R, Zisserman A (2017) Look, listen and learn. ICCV 3, 16

Aytar Y, Vondrick C, Torralba A (2016) Soundnet: Learning sound representations from unlabeled video. In: Advances in Neural Information Processing Systems 3

Bau D, Zhou B, Khosla A, Oliva A, Torralba A (2017) Network dissection: Quantifying interpretability of deep visual representations. CVPR 3

Deng J, Dong W, Socher R, Li LJ, Li K, Fei-Fei L (2009) Imagenet: A large-scale hierarchical image database. In: IEEE Conference on Computer Vision and Pattern Recognition 12

Doersch C, Zisserman A (2017) Multi-task self-supervised visual learning. In: Proceedings of the IEEE Conference on Computer Vision and Pattern Recognition, pp 2051–2060 3

Doersch C, Gupta A, Efros AA (2015) Unsupervised visual representation learning by context prediction. In: IEEE International Conference on Computer Vision 1, 3, 7, 10, 12, 13, 14

Dosovitskiy A, Springenberg JT, Riedmiller M, Brox T (2014) Discriminative unsupervised feature learning with convolutional neural networks. In: Advances in Neural Information Processing Systems 3

Ellis DP, Zeng X, McDermott JH (2011) Classifying soundtracks with audio texture features. In: IEEE International Conference on Acoustics, Speech, and Signal Processing 2, 3

Eronen AJ, Peltonen VT, Tuomi JT, Klapuri AP, Fagerlund S, Sorsa T, Lorho G, Huopaniemi J (2006) Audio-based context recognition. IEEE/ACM Transactions on Audio Speech and Language Processing 14(1):321–329 2

Everingham M, Van Gool L, Williams CK, Winn J, Zisserman A (2010) The pascal visual object classes (voc) challenge. International Journal of Computer Vision 88(2):303–338 12

Fisher III JW, Darrell T, Freeman WT, Viola PA (2000) Learning joint statistical models for audio-visual fusion and segregation. In: Advances in Neural Information Processing Systems 3

Gaver WW (1993) What in the world do we hear?: An ecological approach to auditory event perception. Ecological psychology 5(1):1–29 1, 2, 3

Gemmeke JF, Ellis DP, Freedman D, Jansen A, Lawrence W, Moore RC, Plakal M, Ritter M (2017) Audio set: An ontology and human-labeled dartaset for audio events. In: IEEE International Conference on Acoustics, Speech, and Signal Processing 15

Girshick R (2015) Fast r-cnn. In: IEEE International Conference on Computer Vision 13

Goroshin R, Bruna J, Tompson J, Eigen D, LeCun Y (2015) Unsupervised feature learning from temporal data. arXiv preprint arXiv:150402518 3

Gupta S, Hoffman J, Malik J (2016) Cross modal distillation for supervision transfer. In: Proceedings of the IEEE Conference on Computer Vision and Pattern Recognition 3

Hershey JR, Movellan JR (1999) Audio vision: Using audio-visual synchrony to locate sounds. In: Advances in Neural Information Processing Systems 3

Indyk P, Motwani R (1998) Approximate nearest neighbors: towards removing the curse of dimensionality. In: ACM Symposium on Theory of Computing 5

Ioffe S, Szegedy C (2015) Batch normalization: Accelerating deep network training by reducing internal covariate shift. In: International Conference on Machine Learning 6

Isola P (2015) The discovery of perceptual structure from visual co-occurrences in space and time. PhD thesis 2

Isola P, Zoran D, Krishnan D, Adelson EH (2016) Learning visual groups from co-occurrences in space and time. In: International Conference on Learning Representations, Workshop 3

Jayaraman D, Grauman K (2015) Learning image representations tied to ego-motion. In: IEEE International Conference on Computer Vision 3

Jia Y, Shelhamer E, Donahue J, Karayev S, Long J, Girshick R, Guadarrama S, Darrell T (2014) Caffe: Convolutional architecture for fast feature embedding. In: ACM Multimedia Conference 6

Kidron E, Schechner YY, Elad M (2005) Pixels that sound. In: IEEE Conference on Computer Vision and Pattern Recognition 3

Krähenbühl P, Doersch C, Donahue J, Darrell T (2016) Data-dependent initializations of convolutional neural networks. In: International Conference on Learning Representations 12, 13

Krizhevsky A, Sutskever I, Hinton GE (2012) Imagenet classification with deep convolutional neural networks. In: Advances in Neural Information Processing Systems 6, 13, 14

Le QV, Ranzato MA, Monga R, Devin M, Chen K, Corrado GS, Dean J, Ng AY (2012) Building high-level features using large scale unsupervised learning. In: International Conference on Machine Learning 1

Lee K, Ellis DP, Loui AC (2010) Detecting local semantic concepts in environmental sounds using markov model based clustering. In: IEEE International Conference on Acoustics, Speech, and Signal Processing 2

Leung T, Malik J (2001) Representing and recognizing the visual appearance of materials using three-dimensional textons. International Journal of Computer Vision 43(1):29–44 14

Lin M, Chen Q, Yan S (2014) Network in network. International Conference on Learning Representations 10

McDermott JH, Simoncelli EP (2011) Sound texture perception via statistics of the auditory periphery: evidence from sound synthesis. Neuron 71(5):926–940 1, 2, 4, 16

Mishkin D, Matas J (2015) All you need is a good init. arXiv preprint arXiv:151106422 13

Mobahi H, Collobert R, Weston J (2009) Deep learning from temporal coherence in video. In: International Conference on Machine Learning 3

Ngiam J, Khosla A, Kim M, Nam J, Lee H, Ng AY (2011) Multimodal deep learning. In: International Conference on Machine Learning 3

Oquab M, Bottou L, Laptev I, Sivic J (2015) Is object localization for free?-weakly-supervised learning with convolutional neural networks. In: IEEE Conference on Computer Vision and Pattern Recognition 12

Owens A, Isola P, McDermott J, Torralba A, Adelson EH, Freeman WT (2016a) Visually indicated sounds. In: CVPR 3

Owens A, Wu J, McDermott JH, Freeman WT, Torralba A (2016b) Ambient sound provides supervision for visual learning. In: European Conference on Computer Vision 1, 3

Pathak D, Girshick R, Dollár P, Darrell T, Hariharan B (2017) Learning features by watching objects move. In: CVPR 3, 12, 13

de Sa VR (1994a) Learning classification with unlabeled data. Advances in neural information processing systems pp 112–112 2

de Sa VR (1994b) Minimizing disagreement for self-supervised classification. In: Proceedings of the 1993 Connectionist Models Summer School, Psychology Press, p 300 2

Salakhutdinov R, Hinton G (2009) Semantic hashing. International Journal of Approximate Reasoning 50(7):969–978 5

Slaney M, Covell M (2000) Facesync: A linear operator for measuring synchronization of video facial images and audio tracks. In: Advances in Neural Information Processing Systems 3

Smith L, Gasser M (2005) The development of embodied cognition: Six lessons from babies. Artificial life 11(1-2):13–29 2

Srivastava N, Salakhutdinov RR (2012) Multimodal learning with deep boltzmann machines. In: Advances in Neural Information Processing Systems 3

Thomee B, Shamma DA, Friedland G, Elizalde B, Ni K, Poland D, Borth D, Li LJ (2015) The new data and new challenges in multimedia research. arXiv preprint arXiv:150301817 4, 6

Wang X, Gupta A (2015) Unsupervised learning of visual representations using videos. In: IEEE International Conference on Computer Vision 1, 3, 7, 8, 9, 10, 12, 13, 14

Weiss Y, Torralba A, Fergus R (2009) Spectral hashing. In: Advances in Neural Information Processing Systems 5

Xiao J, Hays J, Ehinger KA, Oliva A, Torralba A (2010) Sun database: Large-scale scene recognition from abbey to zoo. In: IEEE Conference on Computer Vision and Pattern Recognition 6, 12, 14

Zhang R, Isola P, Efros AA (2016) Colorful image colorization. In: European Conference on Computer Vision, Springer, pp 649–666 3, 12, 13

Zhang R, Isola P, Efros AA (2017) Split-brain autoencoders: Unsupervised learning by cross-channel prediction. In: CVPR 3

Zhou B, Lapedriza A, Xiao J, Torralba A, Oliva A (2014) Learning deep features for scene recognition using places database. In: Advances in Neural Information Processing Systems 7, 8, 9, 12, 13, 14

Zhou B, Khosla A, Lapedriza A, Oliva A, Torralba A (2015) Object detectors emerge in deep scene cnns. In: International Conference on Learning Representations 2, 6, 10

Zhou B, Khosla A, Lapedriza A, Oliva A, Torralba A (2016) Learning deep features for discriminative localization. In: The IEEE Conference on Computer Vision and Pattern Recognition (CVPR) 10